

STRATIGRAPHIC ANALYSIS OF THE SOUTH POLAR LAYERED DEPOSITS USING RADAR AND IMAGERY. S. M. Milkovich¹, J. J. Plaut¹, G. Picardi², R. Seu², R. J. Phillips³; Jet Propulsion Laboratory, California Institute of Technology, Pasadena, CA 91109 (Sarah.M.Milkovich@jpl.nasa.gov); INFOCOM Department, University of Rome “La Sapienza,” 00184 Rome, Italy; McDonnell Center for the Space Sciences and Department of Earth and Planetary Sciences, Washington University, St. Louis, MO 63130.

Introduction: The south polar layered deposits (SPLD) are exposed on the walls of troughs and scarps within the south polar deposits of Mars. The details of the formation process of the layers remains unknown; the stratigraphic record and the internal structure of the SPLD can provide clues to these processes. There is evidence for locally continuous layers in regions around the deposit [1-4] and a dome-shaped internal structure rather than horizontal layers [1, 3, 4].

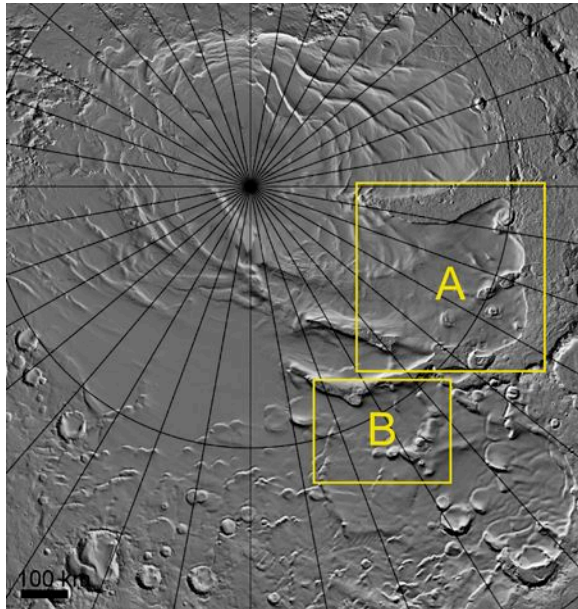


Figure 1: Locations of two regions under analysis.

Recently, two radar instruments have begun collecting information about the subsurface of the polar regions. The MARSIS sounding radar onboard Mars Express (operating at 1.8-5 MHz, [5]) is able to penetrate through the stack of layers and reflect off of the contact with the basement material. The strength of this basal reflection indicates that the material of the SPLD is almost pure water ice [5]. Both MARSIS and SHARAD, the radar onboard Mars Reconnaissance Orbiter (operating at 20 MHz, [6]), detect subsurface reflections at multiple depths within the SPLD in several locations [5, 7]. These reflections could be caused by individual layers or by packets of layers [8], or they could be interference patterns caused by the scale of the SPLD layering.

In this study, we first examine the stratigraphy of two regions (Figure 1) in the radar datasets. We then test the hypothesis that the radar reflections are due to individual layers or packets of layers by examining the layer stratigraphy exposed along the track of multiple orbits of MARSIS data in THEMIS images and attempting to correlate the layers in the visual images with the reflections in the radar.

Radar Stratigraphy. It is important to note that the radargrams shown here display radar returns in time and not distance; to convert to distance requires assumptions about the material the radar is passing through. We calculate elevation measurements assuming a dielectric constant of 3, consistent with pure ice. In the radargrams shown, distance scale bars are calculated in this way, and only apply to the portion of the radargram corresponding to the SPLD. Since the distances scale by the inverse of the square root of the dielectric constant, small variations in material (i.e., dust content) are not likely to have a profound effect on the elevations calculated here. When examining the MARSIS radargrams visually, it is also important to be aware that they are not visually representative of the surface topography due to ionospheric effects; understanding how the depth of a reflection varies along the radargram requires measuring the time delay between the surface reflection and a subsurface reflection on a echo-by-echo basis.

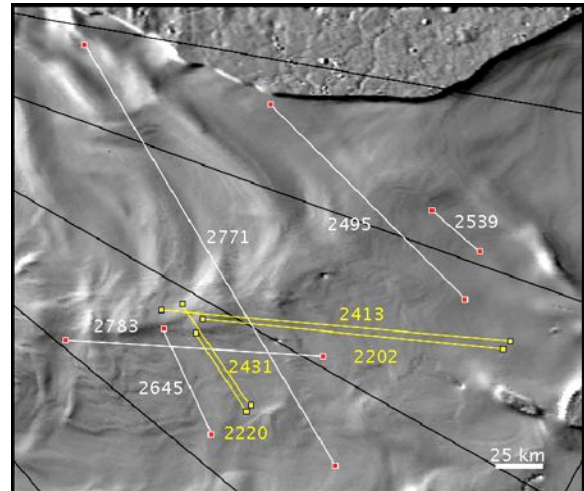


Figure 2: Locations of internal reflections in radar analyzed in Region A. Yellow indicates SHARAD orbits; white with red dots indicates MARSIS orbits.

Region A. Five orbits of MARSIS data and four orbits of SHARAD data were analyzed (Figure 2).

Up to three internal (i.e., not surface or basal) reflections are observed in the MARSIS data (Figure 3). Reflections where orbits cross (2645, 2783, and 2771) are at the same elevations in each radargram (within 100 m, or the resolution of the data) and the reflections in the remaining orbits are at similar elevations; we therefore conclude that the same reflectors are being observed in each orbit.

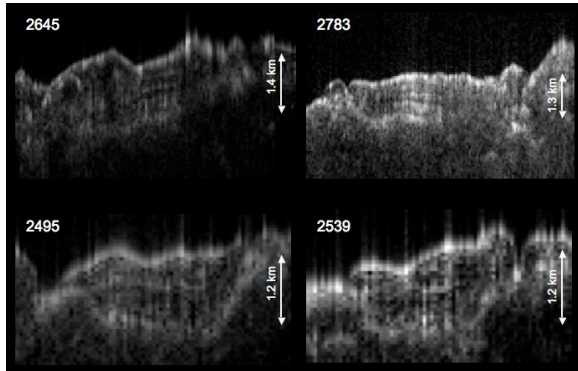


Figure 3. Four MARSIS radargrams from Region A.

Many tens of internal reflections are observed in the SHARAD radargrams (Figure 4). Multiple reflections are traceable over distances of 50 to 150 km in individual radargrams. There are several packets of multiple reflections separated by non-reflective regions with depth. Orbits 2431 and 2413 contain reflections that are correlateable at the location at which they cross; therefore we conclude that the same reflectors are appearing in each radargram. The deepest observable reflection in each SHARAD radargram is at a shallower depth than the deepest reflection in the MARSIS radargrams and

thus the lack of any deeper reflectors is more likely due to attenuation of the radar signal rather than the interface between the base of the SPLD and the underlying plains.

SHARAD orbits 2202 and 2413 contain reflections that are not continuous across the entire radargram; rather, several reflections pinch out in the middle section of the radargram (green line in Figure 5) while other reflections begin in the upper right section of the radargram. This is consistent with two units of layered material separated by an angular unconformity. The upper proposed unit is indicated by the yellow lines in Figure 5 (unit 2). Orbits 2431 and 2220 both cover a shorter distance along the orbit track and do not contain reflections that pinch out.

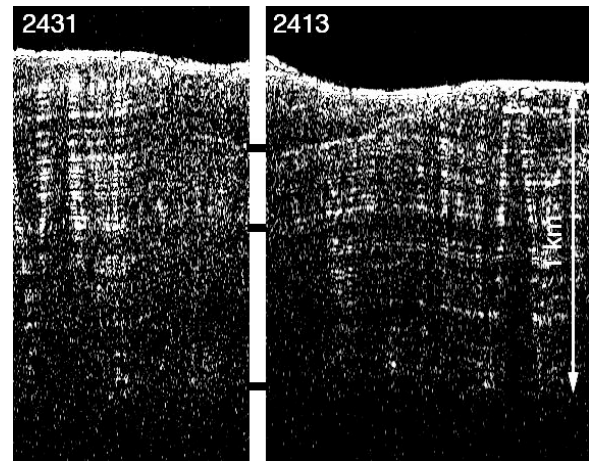


Figure 4: Crossing SHARAD orbits 2431 and 2413. Reflections correlate at the crossing point, -83.6°N, 121.5°E. Scale bar applies to both radargrams.

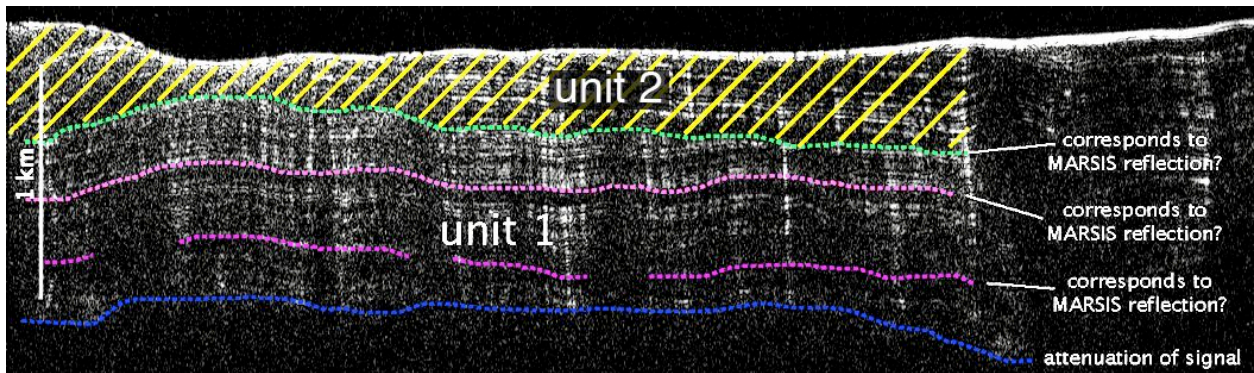


Fig. 5: SHARAD radargram, orbit 2413, indicating two units separated by an angular unconformity and reflections tentatively identified as correlating to MARSIS reflections. The deepest observable reflection is shallower than the deepest reflection in the MARSIS radargrams and thus is not due to the base of the SPLD.

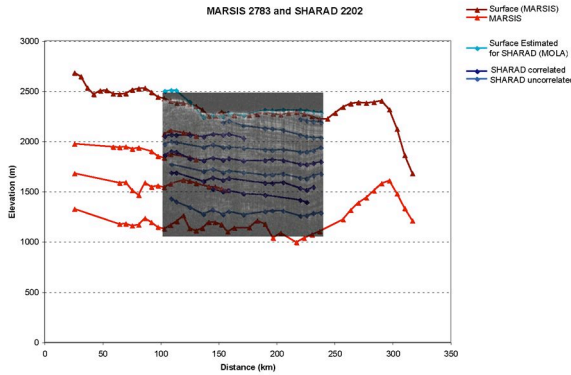


Figure 6: Comparison of SHARAD orbit 2202 and MARSIS orbit 2783. MARSIS data are in red, SHARAD data are in blue.

Neighboring orbits of SHARAD and MARSIS reflections are compared in Figure 6. The MARSIS reflections are at depths that correspond to a transition between a series of reflections and a dark region in the SHARAD radargrams. The same result is found for SHARAD orbit 2220 and MARSIS orbit 2711. Thus, our initial interpretation is that the MARSIS reflections have the same underlying cause in the SPLD layer sequence as the boundaries of the packets of SHARAD reflections. These boundaries are highlighted in Figure 5; however, the reflections are not seen over the same distance in the MARSIS data as they are in the SHARAD data.

Region B. Four orbits of MARSIS data were analyzed in Region B (Figure 7). Internal reflections have also been identified in several SHARAD radargrams; analysis of these data is underway.

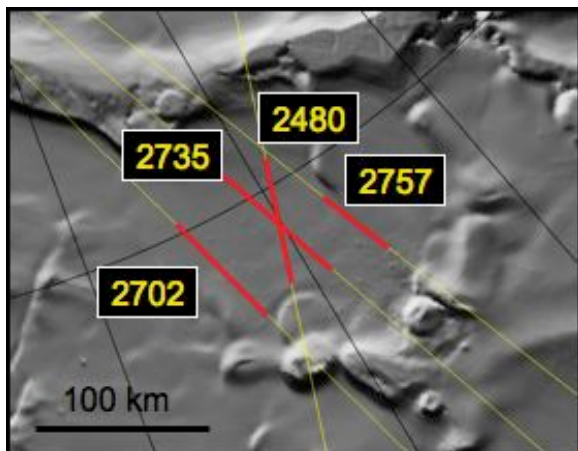


Figure 7: Locations of MARSIS orbits analyzed in Region B. Red lines indicate locations of subsurface reflections.

Similar to Region A, three internal reflections are observed in each MARSIS radargram (Figure 8). Reflections where orbits cross (2480 and 2735) are at

the same elevations in each radargram (within 100 m, or the resolution of the data) and the reflections in the remaining orbits are at similar elevations; we therefore conclude that the same reflectors are being observed in each orbit.

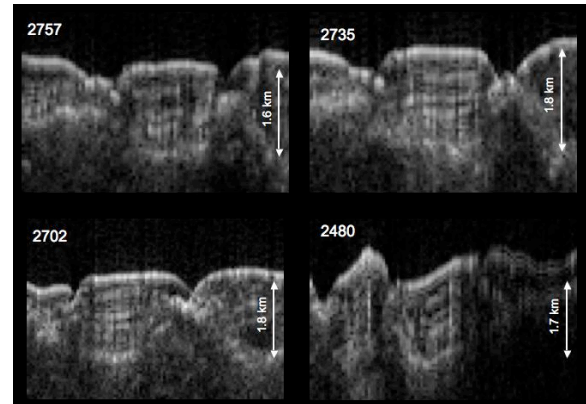


Figure 8: Four MARSIS radargrams from Region B.

Correlating Regions A and B. Stratigraphic analysis of the SPLD layer sequences exposed in THEMIS visible (17 m/pxl) images indicates that there are multiple correlateable marker layers throughout these two regions, and we conclude that the same sequence of layers is found in both regions [3, 4, Figure 9]. If we assume that the internal reflections are due to changing physical properties of the SPLD layer sequence, as is the case for internal reflections observed in terrestrial ice sheets [e.g., 9 and the references therein], then the radar reflections observed in both regions ought to correlate as well. Three MARSIS reflections are observed in both regions, but these reflections do not occur in distinctive patterns that can be definitively correlated.

We will test our hypothesis by comparing the SHARAD reflections observed in both regions.

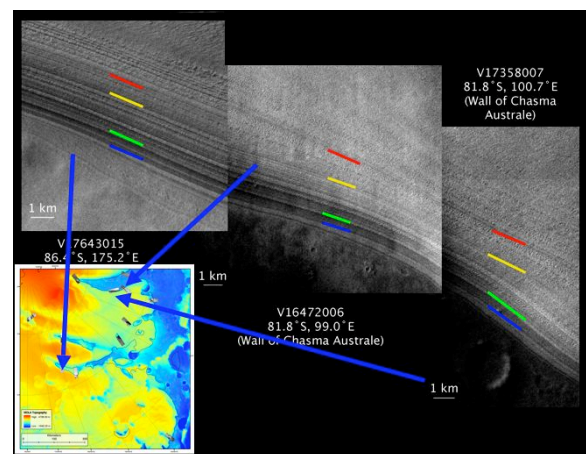


Figure 9: Packets of layers which correlate between Region A and Region B in THEMIS Vis (17 m/pxl) images.

Comparisons with Visual Stratigraphy. In order to determine if the cause of the radar reflections can be found in the images of the SPLD, we first attempted to correlate reflections in MARSIS with individual layers in MOC (1.7 m/pxl) images. Distinctive individual layers are observed in the elevation ranges of each radar reflection, including an unusually thick layer and several erosion-resistant layers. However, if the reflections are due to individual erosion-resistant layers, then similar such layers located elsewhere in the stratigraphic column should also produce reflections. Since these additional surfaces are not observed, we conclude that it is more likely that the reflections are due to packets of layers [7]. We therefore turn to THEMIS visible images (17 m/pxl), which we have found are a useful resolution for examining packets of layers and for conducting stratigraphic analyses [4].

Images were found of layer exposures on polar scarps along the radar groundtracks on either side of the observed internal reflections. The layer sequences in these images were correlated using a series of marker beds (e.g., Figure 9) and the elevations of the correlated marker beds were determined by combining the images with MOLA gridded topography data.

Two methods were used to estimate the elevation of the marker beds away from the polar scarps. The first assumes that the layers were deposited in a non-horizontal plane and that the observed topography of the region was produced by later erosion; this is represented by dashed lines in Figure 10. The second assumes that each layer was draped over a pre-existing deposit from a previous episode of SPLD formation, and the observed topography is produced by a build-up of layers. This is represented by solid lines in Figure 10. The red lines correspond to a distinctive dark layer sequence observed in each image (including those in Figure 9) towards the base of the SPLD exposure.

In the six radargrams analyzed (three in each region), the lower internal reflection is at comparable elevations to the dark layer sequence assuming that the layers follow a plane, while the middle reflection is at comparable elevations if the layers are assumed to be at constant depth throughout the regions. We therefore conclude that this layer sequence *may* correlate with one of the MARSIS reflections, although we cannot as yet conclude which one. Comparisons with the SHARAD reflections may provide further insight.

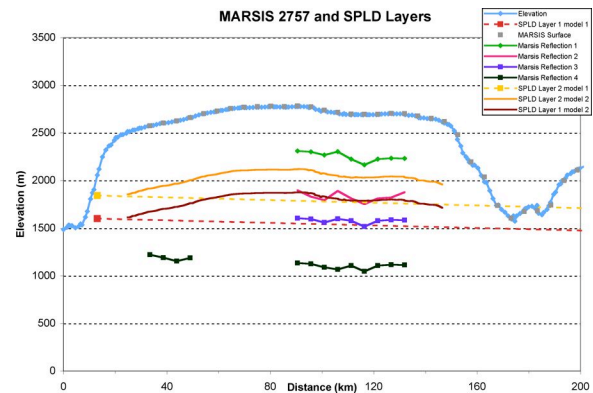


Figure 10. MARSIS reflections in orbit 2757 (green, pink, purple, and dark green lines) with endmember elevation of marker layers (dashed red and yellow lines indicate layers following a non-horizontal plane; solid red and yellow lines indicate layers at a constant depth below the surface).

Conclusions: Analysis of radar data in multiple wavelengths reveals a number of internal reflections within the SPLD. Reflections correlate between orbits within both regions under analysis, and may correlate between regions. The MARSIS reflections may be related to the boundaries of the packets of reflections observed in SHARAD. The angular unconformity observed in the SHARAD dataset is evidence for two distinct episodes of SPLD formation separated by a period of erosion. We have made a tentative correlation between a distinctive packet of layers found in THEMIS images and one of the MARSIS reflections.

Acknowledgments. Thanks to the MARSIS and SHARAD radar teams, especially Ali Safaeinili and Anton Ivanov.

References: [1] S. Byrne and A. Ivanov (2004) *JGR* 109, 10.1029/2004JE002267. [2] E. Kolb and K. Tanaka (2006) *Mars* 2, doi:10.1555/mars.2006.0001. [3] S. Milkovich and J. Plaut (2006), *4th Int. Mars Polar Conf.*, 8092. [4] S. Milkovich and J. Plaut (2007), *LPSC* 38, 1929 [5] J. Plaut et al (2007) *Science* 315 doi:10.1126/science.1139672. [6] R. Seu et al (2004) *Planet. Space Sci.* 52, 157-166. [7] S. Milkovich and J. Plaut (2007), *LPSC* 38, 1816. [8] D. Nunes et al (2006) *LPSC* 37, 1450. [9] J. Dowdeswell and S. Evans (2004) *Rep Prog Phys* 67, 1821-1861.